Chemistry & Biology, Vol. 9, 391–397, March, 2002, ©2002 Elsevier Science Ltd. All rights reserved. PII S1074-5521(02)00109-6

Using an Azobenzene Cross-Linker to Either Increase or Decrease Peptide Helix Content upon *Trans*-to-*Cis* Photoisomerization

Daniel G. Flint,[1,4] Janet R. Kumita,[2,4] Oliver S. Smart,[1] and G. Andrew Woolley[2,3]
[1]School of Biosciences
University of Birmingham
Edgbaston
Birmingham B15 2TT
United Kingdom
[2]Department of Chemistry
University of Toronto
80 Street George Street
Toronto M5S 3H6
Canada

Summary

Reversible photocontrol of peptide and protein conformation could prove to be a powerful tool for probing function in diverse biological systems. Here, we report reversible photoswitching of the helix content in short peptides containing an azobenzene cross-linker between cysteine residues at positions i, i + 4, or i, i + 11 in the sequence. *Trans*-to-*cis* photoisomerization significantly increases the helix content in the i, i + 4 case and significantly decreases the helix content in the i, i + 11 case. These cross-linker designs significantly expand the possibilities for photocontrol of peptide and protein structure.

Introduction

Optical control of peptide/protein conformation can be a powerful biochemical tool for probing protein function in diverse systems [1–4]. Chromophores, such as azobenzene, that undergo reversible *cis-trans* photoisomerization, can, in principle, be used for reversible conformational control of proteins [5–7]. We are interested primarily in designs that can operate in water and that are simple enough to allow the mechanism of the photocontrol to be understood in structural terms. In this way, the design might be transferable and could be used to control a wide variety of proteins. Moroder, Chmielewski, and colleagues have incorporated azobenzene groups directly into the backbone of cyclic peptides [8–11] and have studied the conformational effects of photoisomerization in these systems. Conformational effects of azobenzene-containing side chains have also been studied [12–16].

Recently, we reported a reversible means of controlling helix stability that involved the incorporation of a photoisomerizable azobenzene cross-linking reagent (**1**) into an engineered peptide system [17]. A thiol-reactive azobenzene cross-linker was combined with a peptide containing Cys residues spaced at positions i, i + 7 in the sequence. This design (designated JRK-7-X) was based on molecular modeling studies that indicated that the azobenzene cross-linker in the *trans* conformation was too long to allow the i, i + 7 residues and intervening residues to adopt an α helix conformation. When the cross-linker was in the *cis* conformation, its length better matched the spacing of i, i + 7 residues in an ideal α helix, and it would thus be expected to act as an entropic helix stabilizer. Since Cys residues can be introduced via site-directed mutagenesis into proteins, this azobenzene-based cross-linker strategy offers a general way of photocontrolling protein conformation (and thereby activity).

In general, the dark-adapted state of azobenzene is >99% *trans* isomer [9, 18], whereas the percentage of *cis* isomer that can be achieved upon irradiation is typically 70%–90% depending on the system. This fact sets intrinsic limits on the extent of the photocontrol of protein activity that may be possible using azobenzene. If the *trans* form is active, a 10-fold change in the concentration of the active species is possible (e.g., from >99% *trans* in the dark to 10% *trans* upon irradiation). However, if the *cis* form is the active form, a larger change in the concentration of the active species is possible (e.g., from <1% in the dark to 90% upon irradiation). To maximize photoswitching, one would likely want to have the dark-adapted state as the inactive state of the system. This may correspond to having the *trans* form of the cross-linker stabilize or destabilize a helix, depending on the structure of the target system.

We have applied our molecular modeling strategy in designing further versions of cross-linked peptides that significantly extend the versatility of this approach to the photocontrol of protein structure. Using improved molecular modeling methods, peptides with Cys spacings at i, i + 4 and i, i + 11 were designed, synthesized, and evaluated. We find that the i, i + 4 arrangement leads to a relatively disordered peptide in the dark-adapted state and a large increase in the helix content upon irradiation at 370 nm (*trans*-to-*cis* isomerization), a change similar to that seen with an i, i + 7 spacing for the JRK-7-X peptide. In contrast, the i, i + 11 system is highly helical in the dark-adapted state, and the helix content decreases dramatically upon irradiation at 370 nm (*trans*-to-*cis* isomerization).

Results and Discussion

Peptide Design

A combined quantum mechanics and molecular mechanics (QM/MM) approach was employed to assess the energetic cost of fitting the cross-linker (**1**) in *cis* and *trans* forms to helical peptides with different Cys spacings. It was expected that, if a significant difference existed between the compatibility of *cis* and *trans* conformations of the cross-linker with a helical geometry, photoswitching of peptide conformation would be observed. The relative energies predicted by this modeling approach are presented in Figure 1. The graph shows the calculated potential energy of the *trans* form of the

[3]Correspondence: awoolley@chem.utoronto.ca
[4]These authors contributed equally to this work.

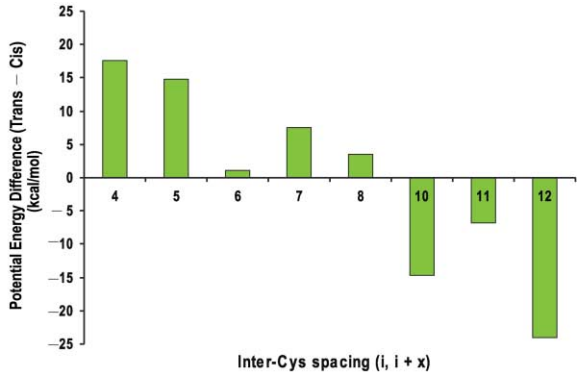

Figure 1. Compatibility of *Cis* versus *Trans* Cross-Linkers with Different Cys Spacings

The potential energy difference is calculated by taking the energy of the *trans* conformation and subtracting the energy of the *cis* conformation for each Cys pair spacing investigated. A positive energy difference implies that, for that Cys spacing, a peptide with a *cis* cross-linker will be more helical than when the linker is *trans*. A negative energy difference implies the opposite: that a peptide will be more helical when the linker is in the *trans* form than when in the *cis* form.

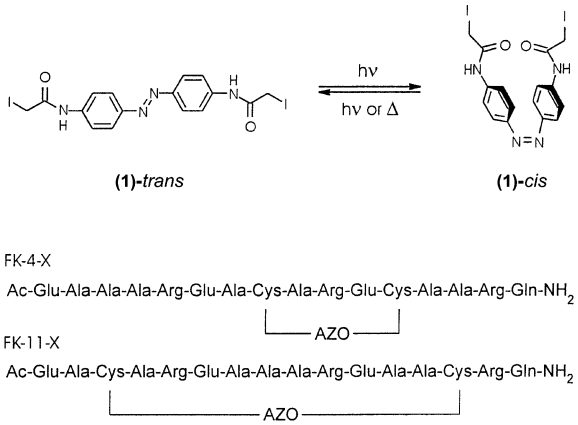

Figure 2. Structures of Peptide Variants and Azobenzene Reagents

A structure of the azobenzene cross-linking reagent and primary sequences of the cross-linked peptides; AZO refers to the cross-linker (**1**) after reaction with the two cysteine side chains.

cross-linker minus that of the *cis* form for each Cys spacing. A positive energy difference implies that a *cis* cross-linker is more compatible with the helical geometry of the peptide than is a *trans* cross-linker. A negative energy difference implies the opposite: a *trans* cross-linker is more compatible with the helix.

As expected, based on our previous work [17], the *cis* form of the cross-linker is more compatible with an i, i + 7 Cys spacing (two helical turns) than is the *trans* form of the cross-linker. This leads to an increase in peptide helical content upon *trans* to *cis* photoisomerization [17]. For Cys spacings of i, i + 4 through i, i + 8, a peptide cross-linked by the *cis* isomer is predicted to be more helical than the *trans* form (Figure 1). Of these spacings, i, i + 4 and i, i + 5 provided the largest energy differences between *cis* and *trans*. The i, i + 4 *cis* cross-linker had a lower absolute conformational energy than the i, i + 5 case, suggesting that it would fit α-helical peptide geometry better. Thus, the i, i + 4 peptide was selected for further investigation by molecular dynamics (MD). For 5 ns of solvated MD, the *cis* i, i + 4 peptide remained helical. The *trans* i, i + 4 peptide unwound from an initial α helix to an extended backbone conformation in the first 200 ps.

For spacings i, i + 10, i, i + 11, and i, i + 12, the *trans* isomer was predicted to be more helix stabilizing than the *cis* isomer (Figure 1). The absolute conformational energy of the *trans* isomer was very high in the i, i + 12 case, however, and so this peptide was not investigated further. In four separate 5-ns simulations of both the i, i + 10 and the i, i + 11 *trans* cross-linked peptides, the peptide backbone conformation remained helical for the entire duration of the run. This demonstrated that both of these spacings would be effective at stabilizing helicity. The i, i + 11 peptide was selected over the i, i + 10 peptide for several reasons. First, viewed on a helical wheel, the angle between the side chains of residues spaced i, i + 11 ($\sim$15°) is far less than for i, i + 10 ($\sim$90°), so that the linker would not have to twist around the helix. Second, the i, i +11 case cyclizes 1 more residue than i, i + 10, so that an entropic helix-stabilizing effect would occur over 12 residues rather than 11. Third, the *cis* cross-linker is expected to be more helix destabilizing at an i, i + 11 spacing than at an i, i + 10 spacing.

Thus, the Cys spacings of i, i + 4 and i, i + 11 were selected for testing in an experimental model peptide. The peptide sequences to be synthesized were chosen based on the extensive work of Baldwin, Stellwagen, and others showing that short alanine-based peptides of general sequence Ac-$(EAAAK)_3$-A-NH_2 are monomeric and have significant helical content in water [19, 20]. The high alanine content of these peptides, central to their helical propensities [21], makes conformational analysis by routine NMR analysis difficult due to severe signal overlap [22–24]. However, extensive spectroscopic studies using CD, FTIR, and selected NMR methods have shown that the α helix is the predominant secondary structure adopted by these systems, with some fraying at the C- and N-terminal ends [22–28]. Since the CD technique has been used extensively for the determination of *relative* helix content in alanine-based peptides [20, 29, 30] as well as in a wide range of proteins [31–33], we felt that it could be used as a reliable reporter of secondary structural changes that occurred upon photoisomerization. We synthesized two peptides, FK-4 and FK-11 (Figure 2), which are analogs of Ac-$(EAAAR)_3$, with Cys residues at i, i + 4, and i, i + 11 spacings, respectively. Each of the peptides was then treated with the azobenzene cross-linking reagent (**1**) (Figure 2) as described in the Experimental Procedures.

Photocontrol with an i, i + 4 Cys Spacing

Molecular models of peptides with the azobenzene cross-linker attached to Cys residues with an i, i + 4 spacing are shown in Figure 3. The *cis* form of the cross-linker is predicted to be compatible with an α-helical conformation of the peptide, whereas the *trans* form of the cross-linker is too extended for such a spacing. The

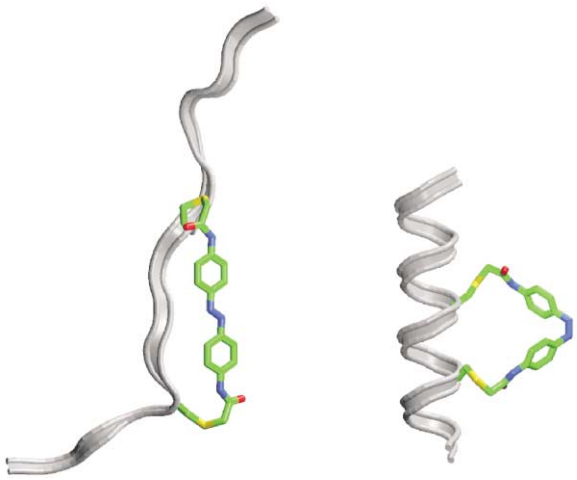

Figure 3. Energy-Optimized Molecular Models of FK-4-X

Schematic models of *trans* FK-4-X (left) and *cis* FK-4-X (right). The peptide backbones are represented by a silver ribbon. The cysteine side chain and cross-linker atoms are colored according to atom type: carbon = green, nitrogen = blue, oxygen = red, and sulfur = yellow. Hydrogens are omitted for clarity. The helical model is the final frame of a 500-ps MD run after starting from a helical conformation. To generate the coil model, the peptide was built in SYBYL, and a random backbone conformation was generated. The cross-linker was then attached to the peptide, and the complete molecule was subjected to energy minimization, with the linker atoms constrained to their initial positions. A further round of energy minimization was then undertaken with all atoms free to move.

trans form of the cross-linked FK-4-X peptide is thus expected to unfold in solution.

The UV/Vis absorption spectrum of the dark-adapted (*trans*) form of the cross-linked FK-4-X peptide in aqueous solution is shown in Figure 4A (solid line). The absorption maximum occurs near 370 nm, typical for an amide-substituted azobenzene $\pi-\pi^*$ transition [18]. Irradiation of the peptide solution with 370-nm light for 5 min ($\sim$5 mW) produces a solution that is 90% $\pm$ 3% *cis* isomer (Figure 4A, dotted line). The spectrum of the pure *cis* form of the chromophore (obtained as described in the Experimental Procedures) is shown for reference (Figure 4A, dash-dot line). The absorbance change is fully reversible in the dark, with a half-time of about 36 min at 25°C and 6 min at 37°C (Table 1). These half-lives are longer than those observed previously in our study of the thermal *cis-trans* isomerization of the JRK-7-X peptide (Table 1), especially at 25°C.

The secondary structure of the FK-4-X peptide was investigated using circular dichroism (CD) spectroscopy. Figure 4B (solid line) shows the circular dichroism spectrum of the dark-adapted cross-linked peptide with the azo group in the *trans* conformation. The spectrum is typical of a mixture of disordered structure with a small percentage of helix content [31].

When the cross-linked peptide was irradiated at 370 nm, the intensity of the negative CD band at 222 nm increased significantly (Figure 4B, dotted line), the minimum at 202 nm shifted to 207 nm, and the intensity of the maximum at 190 nm increased significantly. The spectrum of the *cis* peptide was thus characteristic of an α helix (minima at 222 nm and 208 nm, maximum at

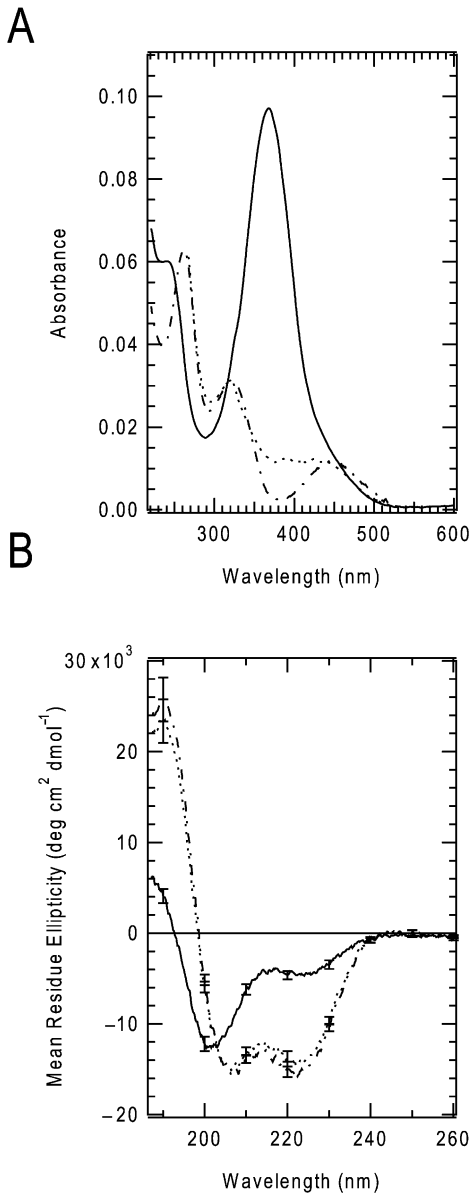

Figure 4. Effects of Photoirradiation on Secondary Structure of FK-4-X

(A) UV/Vis spectrum of FK-4-X (35 μM, 5 mM phosphate buffer [pH 7.0]) in the dark-adapted state (solid line) and after irradiation at 370 nm (dotted line). The spectrum of the pure *cis* chromophore is shown as a dash-dot line.

(B) CD spectrum of FK-4-X (35 μM, 5 mM phosphate buffer [pH 7.0]) in the dark-adapted state (solid line) and after irradiation at 370 nm (dotted line). The calculated CD spectrum for the 100% *cis* peptide is shown as a dash-dot line.

190 nm), whereas the *trans* peptide was characteristic of a predominantly disordered structure. The corrected spectrum for the 100% *cis* peptide (dash-dot line) was calculated based on the observed percentage conversion by UV/Vis spectroscopy (see above).

The magnitude of the change in the CD spectrum of the cross-linked peptide upon photoisomerization is dependent on temperature. Lower temperatures result in larger changes, primarily because lower temperatures

Table 1. Half-Lives for Thermal Relaxation of Cross-Linked Peptides

	25°C $\tau_{1/2}$ (min)	37°C $\tau_{1/2}$ (min)
FK-4-X	36.5 ± 0.5	5.9 ± 0.3
JRK-7-X[a]	22 ± 0.5	5.6 ± 0.3
FK-11-X	12.3 ± 0.3	2.5 ± 0.2
Gluthathione-X	12.8 ± 0.3	3.5 ± 0.3

[a] Data from [17].

significantly increase the apparent helix content of the *cis* form of the peptide (data not shown). While differences in θ_{222} indicate changes in the helix content, assignment of a particular value of θ_{222} to a particular percentage helix is more difficult [34]. Using the simple assumption that θ_{222} for the 100% helix is given by 40,000 × ([n − 4]/n), where n is the number of residues [35], the light-induced transition shown in Figure 4B is from the 15%–53% helix. The structural transition observed upon photoisomerization of the cross-linked peptide is fully reversible. If the *cis* form of the peptide is kept in the dark, the CD spectrum of the *trans* form is recovered with a time course that matches, within experimental error, that seen using UV/Vis spectroscopy.

The i, i + 4 spacing thus appears to permit photostimulated increase of helical structure from a largely disordered dark state.

Photocontrol with an i, i + 11 Cys Spacing

Molecular models of peptides with the azobenzene cross-linker attached to Cys residues with an i, i + 11 spacing are shown in Figure 5. In this case, the *trans* form of the cross-linker is predicted to be compatible with an α-helical conformation of the peptide, whereas the *cis* form of the cross-linker is too short to fit such a spacing. The *cis* form of the cross-linked FK-11-X peptide is thus expected to unfold in solution.

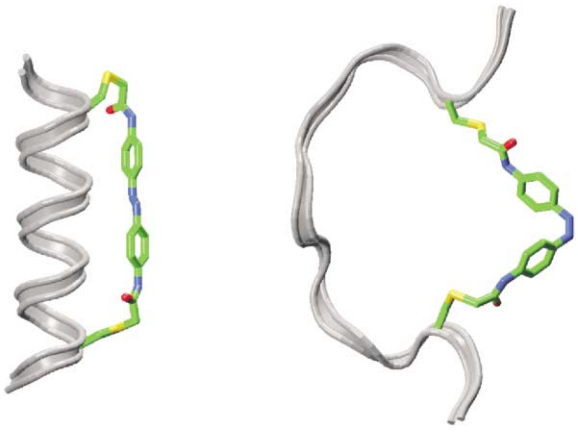

Figure 5. Energy-Optimized Molecular Models of FK-11-X

Schematic models of *trans* FK-11 (left) and *cis* FK-11 (right). The peptide backbones are represented by a silver ribbon. The cysteine side chain and cross-linker atoms are colored according to atom type: carbon = green, nitrogen = blue, oxygen = red, and sulfur = yellow. Hydrogens are omitted for clarity. The helical model is the final frame of a 500-ps MD run after starting from a helical conformation. To generate the coil model, the peptide was built in SYBYL, and a random backbone conformation was generated. The cross-linker was then attached to the peptide, and the complete molecule was subjected to energy minimization, with the linker atoms constrained to their initial positions. A further round of energy minimization was then undertaken with all atoms free to move.

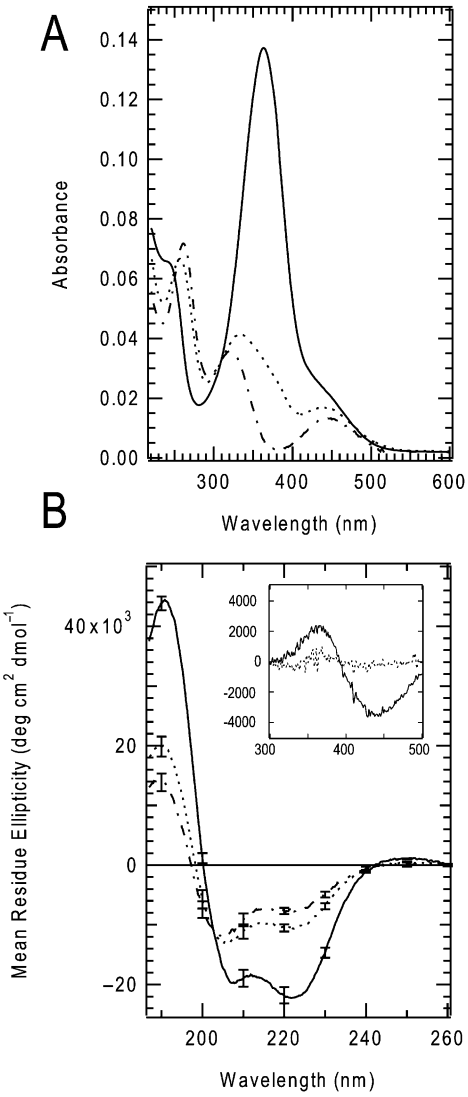

Figure 6. Effects of Photoirradiation on Secondary Structure of FK-11-X

(A) UV/Vis spectrum of FK-11-X (44 μM, 5 mM phosphate buffer [pH 7.0]) in the dark-adapted state (solid line) and after irradiation at 370 nm (dotted line). The spectrum of the pure *cis* chromophore is shown as a dash-dot line.

(B) CD spectrum of FK-11-X (44 μM, 5 mM phosphate buffer [pH 7.0]) in the dark-adapted state (solid line) and after irradiation at 370 nm (dotted line). The calculated CD spectrum for the 100% *cis* peptide is shown as a dash-dot line. Inset: long-wavelength CD spectrum of FK-11-X (44 μM, 5 mM phosphate buffer [pH 7.0]) in the dark-adapted state (solid line) and after irradiation at 370 nm (dotted line).

UV/Vis absorption spectra of the dark-adapted (*trans*) and irradiated forms of the cross-linked FK-11-X peptide in aqueous solution are shown in Figure 6A. Irradiation at 370 nm for 5 min (~5 mW) led to 80% ± 3% of the *cis* isomer. The spectrum of the pure *cis* form of the

chromophore is shown for reference (Figure 4A, dash-dot line). Thermal reversion to the *trans* form is significantly faster than in the FK-4-X case (Table 1). In fact, the half-life for thermal reversion in this case is similar to that observed with the model compound glutathione-X in which the cross-linker is attached to two molecules of glutathione (Table 1). The rate of thermal reversion is related to the energy barrier between the *cis* ground state and the transition state in each case. It is noteworthy that, for *cis* cross-linkers attached to (what are expected to be) disordered peptides, these activation barriers are lower than when the cross-linkers are attached to ordered (helical) peptides.

Figure 6B shows CD spectra obtained for FK-11-X in the dark-adapted (solid line) state and after irradiation (dotted line). Based on the percentage conversion by UV/Vis spectroscopy, a spectrum for the 100% *cis* peptide was calculated (dash-dot line). In direct contrast to the FK-4-X case, the dark-adapted FK-11-X peptide is highly helical (66%). Irradiation causes a substantial decrease in helical content (to 26%). The FK-11-X system thus permits a photostimulated decrease of helical structure from a largely helical dark state.

As with the FK-4-X case, an isodichroic point is observed at 203 nm, indicating the existence of a simple two-state equilibrium between helical and disordered forms of the peptide. We found no evidence of peptide self-association. The same CD change and isodichroic point were observed in solutions of varying peptide concentrations (5–80 μM), and no evidence of light scattering or of β-type secondary structures typical of an aggregated peptide [13, 16] were seen.

Interestingly, the CD spectrum of the dark-adapted FK-11-X peptide shows features not observed with the FK-4-X peptide (or with the JRK-7-X peptide [17]). In particular, the negative band at 222 nm is more pronounced than the band at 208 nm (this is not observed in the FK-4-X spectrum [Figure 4B]). Also, there is a small positive ellipticity at 250 nm in the dark-adapted FK-11-X spectrum. Furthermore, an exciton-type CD signal is observed at longer wavelengths (Figure 6B, inset) in the FK-11-X dark-adapted state and is not observed with FK-4-X (data not shown) and disappears upon irradiation (Figure 6B, inset). This signal is presumably due to transitions in the azobenzene chromophore in which chirality is induced by its proximity to the peptide. Indeed, the models (Figure 5) indicate that the *trans* cross-linker will be tightly packed against the helical FK-11-X peptide and may have hindered rotation. Azobenzene transitions may also account for the extra negative ellipticity at 222 nm and the weak positive band at 250 nm.

Significance

The activities of proteins with key helical domains involved in function, such as leucine zippers and helix-loop-helix transcription factors, and certain proteins involved in signal transduction, might be reversibly photocontrolled using this reagent. Such photocontrolled proteins could be useful for probing the importance of timing in biochemical networks.

Experimental Procedures

Molecular Modeling

Initial models of the cross-linker in *cis* and *trans* conformations were constructed using SYBYL 6.7 (Tripos). These starting structures were then optimized using Gaussian 98 [36] with the B3LYP density functional theory method [37] and the 6-31G* basis set. The B3LYP/6-31G* quantum mechanical (QM) representation has previously been shown to represent the geometry of azobenzene well [38, 39]. Eight 16-residue polyalanine helices were also built in SYBYL, each one containing two Cys that are a specific number of residues apart. The N termini of the peptides were acetylated, and the C termini were amidated. Cys spacings from i, i + 4 to i, i + 12 were investigated. The i, i + 9 spacing was not investigated, because the side chains of these two residues lie on opposite sides of the helix. The peptides were subjected to energy minimization using the AMBER 96 forcefield [40] until convergence was reached.

For each of the eight peptides, the cross-linker was joined to the two Cys residues in either the *cis* or the *trans* state. To investigate multiple conformations of the Cys side chains, the χ_1 angle was set at either 180° (*trans*) or −60° (g+) prior to the cross-linker being attached. For a Cys residue in an α helix, a χ_1 angle of 60° (g−) is sterically unfavorable due to the close contact between the sulfur and the backbone carbonyl of the residue located at the i−3 position [41]. The linker from Cβ to Cβ of each Cys was then subjected to energy minimization using extra parameters incorporated into the AMBER 96 forcefield (parameterization will be described elsewhere), with atoms of the rest of the peptide constrained to their starting positions. Optimization was then repeated using a QM/MM representation as implemented in ROAR 2.0 [42]. The atoms of the linker and the side chains of the Cys were represented by the AM1 Hamiltonian [43]. All other atoms of the peptide were represented by the AMBER 96 forcefield. Only the atoms represented by AM1 were allowed to move; all others were constrained to their original positions.

Finally, a single-point QM potential energy calculation was performed. The peptide was deleted, leaving only the linker and the Cys side chains up to the α carbon. A single-point energy calculation was then performed using the B3LYP method and the 6-31G* basis set using Gaussian 98. This final calculation thus provides an estimate of the energy cost of fitting the linker to a particular Cys spacing of an α helix. The whole process was repeated four times for each linker conformation and each peptide.

Cross-linked peptides with Cys spacings of i, i + 4; i, i + 10; or i, i + 11 were subjected to simulations using the molecular dynamics program Sander Classic from the AMBER 6.0 suite of programs [44]. Each peptide was solvated by a truncated octahedral box of approximately 3000 TIP3P waters [45]. Periodic boundary conditions were used so that solvent molecules would be free to move. A constant dielectric ($\epsilon = 1$) was used. The nonbonded pair list was subjected to a cutoff of 14 Å and updated every 50 steps. The periodic system was then subjected to energy minimization, followed by slow heating from 0K to 297K. This was followed by 100,000 steps of constant pressure equilibration. During the equilibration process, all peptide atoms were restrained to their original positions so that the production run would start with the peptide backbone in an α-helical conformation. For the production run, all restraints were removed, so all atoms in the system were free to move. Each system was simulated for 5 ns with a time integration step of 2 fs.

Synthesis of Azobenzene Cross-Linking Reagent

The azobenzene cross-linking reagent containing two cysteine-reactive iodoacetamide groups (structure **1**) was synthesized as previously reported [17].

Peptide Synthesis

Standard fluorenylmethoxycarbonyl-based solid-phase peptide synthesis methods were used to prepare the two peptides, FK-4: Ac-EAAAREACARECAARQ-NH_2 and FK-11: Ac-EACAREAAARE AACRQ-NH_2. Peptides were constructed on Pal-resin (capacity 0.55 mmol/g) (Advanced ChemTech). Coupling used 3 equivalents HATU (*O*-[7-azobenzotriazol-1-yl]-1,1,3,3-tetramethyluronium hexafluoro-

phosphate) (Sigma-Aldrich Canada), 6 equivalents DIPEA (*N,N*-diisopropylethylamine), and 3 equivalents amino acid (Novabiochem). Peptides were purified by HPLC (Apex Presil C18 8μ column [Jones Chromatography]) using a linear gradient of 0%–80% acetonitrile/H_2O (+0.1% trifluoroacetic acid) over 45 min for FK-4 (eluted at 39.1% acetonitrile) and a gradient of 0%–30% acetonitrile/H_2O (+0.1% trifluoroacetic acid) for 10 min, followed by a gradient of 30%–45% acetonitrile/H_2O (+0.1% trifluoroacetic acid) for 19 min, for FK-11 (eluted at 36% acetonitrile). The peptide primary structures were confirmed by electrospray ionization MS and amino acid analysis (HSC Biotechnology Service Centre); FK-4: observed 1746.3 Da; calculated ($C_{67}H_{115}N_{27}O_{24}S_2$) 1746.9 Da, and FK-11: observed 1746.5 Da; calculated ($C_{67}H_{115}N_{27}O_{24}S_2$) 1746.9 Da. The purity by HPLC was >95%.

Peptide Cross-Linking

Intramolecular cross-linking of Cys residues in FK-11 by **1** was performed as described by Kumita and coworkers [17]. Cross-linked peptides are indicated by an "X" following the peptide identification (e.g., FK-11-X).

For FK-4, the cross-linking procedure was modified due to the uncross-linked peptide being 50% helical. Cross-linking of FK-4 was performed with the cross-linker in the predominantly (helix accommodating) *cis* state. In a total volume of 500 μl 64 mM Tris-Cl buffer (pH 8), uncross-linked FK-4 (0.79 mM) and TCEP (1.19 mM) were combined and incubated for 18 hr at room temperature; this was performed under nitrogen to ensure that the cysteine residues were in their reduced state. A 10 mM solution of **1** (in DMSO) was made and irradiated with 370-nm light (in a 1-cm quartz cuvette) for 10 min. A total of 60 μl of the irradiated 10 mM solution of **1** was combined with 440 μl DMSO. The cross-linker solution was kept at 18°C in an ice-water bath, and the peptide was added, stirred, and exposed to light (Sylvania GRO-LUX Daylight lamp [875 lumens]) for 10 min. The addition of the irradiated solution **1** was repeated three times (at 10-min intervals) for a total reagent concentration of 2.0 mM. The reaction mixture was stirred for an additional 20 min while exposed to ambient light. The solvent was removed from the reaction mixture under high vacuum.

Unreacted **1** was removed by Biogel P4 gel-filtration chromatography, and the peptides were purified by HPLC (Zorbax SB-C18 column) using a linear gradient of 0%–80% acetonitrile/H_2O (+0.1% trifluoroacetic acid) over the course of 45 min for FK-4-X (eluted at 38.8% acetonitrile) and FK-11-X (eluted at 40.9% acetonitrile). The peptide primary structures were confirmed by MALDI MS and amino acid analysis (HSC Biotechnology Service Centre); FK-4-X: observed 2039.0 Da; calculated ($C_{83}H_{127}N_{31}O_{26}S_2$) 2039.2 Da, and FK-11a-X: observed 2038.7 Da; calculated ($C_{83}H_{127}N_{31}O_{26}S_2$) 2039.2 Da.

UV/Vis Analysis and Photoisomerization

UV spectra were obtained with a Perkin-Elmer Lambda 2 spectrophotometer using the same thermostatted quartz cell (0.1-cm pathlength) in which CD analysis was performed. Peptide concentrations of cross-linked species were calculated using a molar extinction coefficient of 28,000 (367 nm) for the dark-adapted azo group.

Photoisomerization was accomplished by irradiating thermostatted peptide solutions with a 70 W Metal Halide Tri-Lite Lamp (World Precision Instruments) coupled to a 370 ± 10-nm band pass filter (Harvard Apparatus Canada). Photoisomerization was complete (as judged by the lack of any further changes in UV spectra) in ≤5 min. Spectra for pure *trans* and *cis* forms of the azobenzene cross-linker were obtained using a Waters 996 photodiode array (PDA) detector coupled to an HPLC system comprised of a Waters 600 series controller and pump (Waters). *Trans* and *cis* isomers of FK-11-X and JRK-7-X were separated on an Alltima C-18 5-μm (250 mm × 4.6 mm) column preceded by an Econosil C-18 10-μm guard cartridge (Alltech). A linear gradient of 20%–70% A over 10 min followed by 70% A for 5 min (where solvent A was 80% acetonitrile/20% water, with 0.1% trifluoroacetic acid) was used. The total concentration of the sample was calculated based on the molar extinction coefficient for the dark-adapted (*trans*) form. By comparing the peak areas at 310 nm (an isosbestic point), the percent of each isomer present in the sample could be determined.

Circular Dichroism Measurements

Circular dichroism measurements were performed with a Jasco Model J-710 spectropolarimeter. All measurements were made in a thermostatted quartz cuvette (0.1-cm pathlength). Temperatures were measured using a microprobe directly in the sample cell. All samples were dissolved in 5 mM phosphate buffer (pH 7.0). Spectra reported are averages of three individual experiments of five scans each, with the appropriate background spectrum subtracted. A scan speed of 10 nm/min, with a 0.5-nm band width and a 4-s response time, was used. The mean residue weight used for both FK-4-X and FK-11-X was 109.1. Using the percent *cis* observed by UV/Vis, theoretical 100% *cis* CD spectra were calculated using Equation 1:

$$\theta(100\%\ cis) = [\theta(\text{observed after irradiation}) - (\text{fraction } trans \times \theta\ (\text{dark-adapted}))]/\text{fraction } cis. \quad (1)$$

Helix content was calculated by using the simple assumption that the 100% helix gives a θ_{222} value of 40,000 × ([n − 4]/n), where n is the number of residues [46]. In the case of the *trans* CD spectrum of FK-11-X, θ_{208} was substituted for θ_{222} in this expression due to a contribution to θ_{222} from the azobenzene chromophore (see Results and Discussion).

Acknowledgments

We would like to acknowledge Natural Sciences and Engineering Research Council (NSERC) (Canada) (G.A.W.), the Volkswagen Stiftung (Germany) (G.A.W.), and the United Kingdom Medical Research Council (grant G.4600017 [O.S.S.]) for financial support. J.R.K. was supported by an NSERC and a Dr. Dina Gordon Malkin/OGSST studentship. D.G.F. was supported by a United Kingdom Medical Research Council Bioinformatics studentship.

Received: August 21, 2001
Revised: December 4, 2001
Accepted: January 8, 2002

References

1. Adams, S.R., and Tsien, R.Y. (1993). Controlling cell chemistry with caged compounds. Annu. Rev. Physiol. *55*, 755–784.
2. Curley, K., and Lawrence, D.S. (1999). Light-activated proteins. Curr. Opin. Chem. Biol. *3*, 84–88.
3. Miller, J.C., Silverman, S.K., England, P.M., Dougherty, D.A., and Lester, H.A. (1998). Flash decaging of tyrosine side chains in an ion channel. Neuron *20*, 619–624.
4. Pan, P., and Bayley, H. (1997). Caged cysteine and thiophosphoryl peptides. FEBS Lett. *405*, 81–85.
5. Liu, D., Karanicolas, J., Yu, C., Zhang, Z., and Woolley, G.A. (1997). Site-specific incorporation of photoisomerizable azobenzene groups into ribonuclease S. Bioorg. Med. Chem. Lett. *7*, 2677–2680.
6. Hamachi, I., Hiraoka, T., Yamada, Y., and Shinkai, S. (1998). Photoswitching of the enzymatic activity of semisynthetic ribonuclease S bearing phenylazophenylalanine at a specific site. Chem. Lett. *6*, 537–538.
7. Willner, I., and Rubin, I. (1996). Control of the structure and functions of biomaterials by light. Angew. Chem. Int. Ed. Engl. *35*, 367–385.
8. Renner, C., Cramer, J., Behrendt, R., and Moroder, L. (2000). Photomodulation of conformational states. II. Mono- and bicyclic peptides with (4-aminomethyl) phenylazobenzoic acid as backbone constituent. Biopolymers *54*, 501–514.
9. Renner, C., Behrendt, R., Sporlein, S., Wachtveitl, J., and Moroder, L. (2000). Photomodulation of conformational states. I. Mono- and bicyclic peptides with (4-amino)phenylazobenzoic acid as backbone constituent. Biopolymers *54*, 489–500.
10. Ulysse, L., Cubillos, J., and Chmielewski, J. (1995). Photoregulation of cyclic peptide conformation. J. Am. Chem. Soc. *117*, 8466–8467.
11. Behrendt, R., Renner, C., Schenk, M., Wang, F., Wachtveitl, J., Oesterhelt, D., and Moroder, L. (1999). Photomodulation of the

conformation of cyclic peptides with azobenzene moieties in the peptide backbone. Angew. Chem. Int. Ed. Engl. *38*, 2771–2774.
12. Cooper, T.M., Natarajan, L.V., and Crane, R.L. (1993). Light-responsive polypeptides. Trends Polym. Sci. *1*, 400–405.
13. Pieroni, O., Fissi, A., Houben, J.L., and Ciardelli, F. (1985). Photo-induced aggregation changes in photochromic polypeptides. J. Am. Chem. Soc. *107*, 2990–2991.
14. Pieroni, O., and Ciardelli, F. (1995). Photoresponsive polymeric materials. Trends. Polym. Sci. *3*, 282–287.
15. Zhang, J., James, D.A., and Woolley, G.A. (1999). PATIC: a conformationally constrained photoisomerizable amino acid. J. Pept. Res. *53*, 560–568.
16. Cerpa, R., Cohen, F.E., and Kuntz, I.D. (1996). Conformational switching in designed peptides: the helix/sheet transition. Fold. Des. *1*, 91–101.
17. Kumita, J.R., Smart, O.S., and Woolley, G.A. (2000). Photo-control of helix content in a short peptide. Proc. Natl. Acad. Sci. USA *97*, 3803–3808.
18. Rau, H. (1990).Photoisomerization of azobenzenes. In Photochemistry and Photophysics, J.F. Rabek, ed. (Boca Raton, FL: CRC Press), pp. 119–141.
19. Marqusee, S., Robbins, V.H., and Baldwin, R.L. (1989). Unusually stable helix formation in short alanine-based peptides. Proc. Natl. Acad. Sci. USA *86*, 5286–5290.
20. Merutka, G., and Stellwagen, E. (1990). Positional independence and additivity of amino acid replacements on helix stability in monomeric peptides. Biochemistry *29*, 894–898.
21. Rohl, C.A., Fiori, W., and Baldwin, R.L. (1999). Alanine is helix-stabilizing in both template-nucleated and standard peptide helices. Proc. Natl. Acad. Sci. USA *96*, 3682–3687.
22. Merutka, G., Morikis, D., Bruschweiler, R., and Wright, P.E. (1993). NMR evidence for multiple conformations in a highly helical model peptide. Biochemistry *32*, 13089–13097.
23. Venyaminov, S.Y., Hedstrom, J.F., and Prendergast, F.G. (2001). Analysis of the segmental stability of helical peptides by isotope-edited infrared spectroscopy. Proteins *45*, 81–89.
24. Millhauser, G.L., Stenland, C.J., Bolin, K.A., and van de Ven, F.J. (1996). Local helix content in an alanine-rich peptide as determined by the complete set of 3JHN alpha coupling constants. J. Biomol. NMR *7*, 331–334.
25. Huang, C.Y., Klemke, J.W., Getahun, Z., DeGrado, W.F., and Gai, F. (2001). Temperature-dependent helix-coil transition of an alanine based peptide. J. Am. Chem. Soc. *123*, 9235–9238.
26. Williams, L., Kather, K., and Kemp, D. (1998). High helicities of Lys-containing, Ala-rich peptides are primarily attributable to a large, context-dependent Lys stabilization. J. Am. Chem. Soc. *120*, 11033–11043.
27. Pastrana-Rios, B. (2001). Mechanism of unfolding of a model helical peptide. Biochemistry *40*, 9074–9081.
28. Shalongo, W., Dugad, L., and Stellwagen, E. (1994). Analysis of the thermal transitions of a model helical peptide using C-13 NMR. J. Am. Chem. Soc. *116*, 2500–2507.
29. Chakrabartty, A., and Baldwin, R.L. (1995). Stability of alpha-helices. Adv. Protein Chem. *46*, 141–176.
30. Marqusee, S., and Baldwin, R.L. (1987). Helix stabilization of Glu^{-}— Lys^{+} salt bridges in short peptides of *de novo* design. Proc. Natl. Acad. Sci. USA *84*, 8898–8902.
31. Johnson, W.C., Jr. (1990). Protein secondary structure and circular dichroism: a practical guide. Proteins *7*, 205–214.
32. Greenfield, N.J. (1996). Methods to estimate the conformation of proteins and polypeptides from circular dichroism data. Anal. Biochem. *235*, 1–10.
33. Woody, R.W. (1995). Circular dichroism. Methods Enzymol. *246*, 34–71.
34. Wallimann, P., Kennedy, R.J., and Kemp, D.S. (1999). Large circular dichroism ellipticities for N-templated helical polypeptides are inconsistent with currently accepted helicity algorithms. Angew. Chem. Int. Ed. Engl. *38*, 1290–1292.
35. Jackson, D., King, D., Chmielewski, J., Singh, S., and Schultz, P. (1991). General approach to the synthesis of short α-helical peptides. J. Am. Chem. Soc. *113*, 9391–9392.
36. Frisch, A., Hammer, R.P., Schlegel, H.B., Scuseria, G.E., Robb, M.A., Cheeseman, J.R., Zakrzewski, V.G., Montgomery, J.A., Stratmann, R.E., Burant, J.C., et al. (1998). Gaussian *98* (Pittsburgh: Gaussian).
37. Becke, A.D. (1997). Density functional thermochemistry 3. The role of exact exchange. J. Chem. Phys. *98*, 5648–5652.
38. Biswas, N., and Umapathy, S. (1997). Density functional calculations of structures, vibrational frequencies, and normal modes of trans- and cis-azobenzene. J. Phys. Chem. A *101*, 5555–5566.
39. Kurita, N., Tanaka, S., and Itoh, S. (2000). Ab initio molecular orbital and density functional studies on the stable structures and vibrational properties of trans- and cis- azobenzenes. J. Phys. Chem. A *104*, 8114–8120.
40. Cornell, W.D., Cieplak, P., Bayly, C.I., Gould, I.R., Merz, K.M., Ferguson, D.M., Spellmeyer, D.C., Fox, T., Caldwell, J.W., and Kollman, P.A. (1995). A second generation force field for the simulation of proteins, nucleic acids, and organic molecules. J. Am. Chem. Soc. *117*, 5179–5197.
41. Stapley, B.J., and Doig, A.J. (1997). Free energies of amino acid side-chain rotamers in alpha-helices, beta-sheets and alpha-helix N-caps. J. Mol. Biol. *272*, 456–464.
42. Cheng, A., Stanton, R.S., Vincent, J.J., van der Vaart, A., Damodaran, K.V., Dixon, S.L., Hartsough, D.S., Mori, M., Best, S.A., Monard, G., et al. (1999). The ROAR 2.0 Program (State College, PA: Pennsylvania State University).
43. Dewar, M.J.S., Zoebisch, E.G., Healy, E.F., and Stewart, J.J.P. (1985). AM1: a new general purpose quantum mechanical molecular model. J. Am. Chem. Soc. *107*, 3902–3909.
44. Kollman, P. (2000). Amber 6.0. (San Francisco: University of California, San Francisco).
45. Jorgensen, W.L. (1981). Quantum and statistical mechanical studies of liquids 10. Transferable intermolecular potential functions for water, alcohols, and ethers - application to liquid water. J. Am. Chem. Soc. *103*, 335–340.
46. Kallenbach, N.R., and Spek, E.J. (1998). Modified amino acids as probes of helix stability. Methods Enzymol. *295*, 26–41.